Geochemical Journal, Vol. 48, pp. 433 to 449, 2014 doi:10.2343/geochemj.2.0320

Regional mantle heterogeneity regulates melt production along the Réunion hotspot-influenced Central Indian Ridge

Shiki Machida,[1,2]* Yuji Orihashi,[3] Marco Magnani,[3,4] Natsuki Neo,[5] Samantha Wilson,[6] Masaharu Tanimizu,[7] Shigekazu Yoneda,[8] Atsushi Yasuda[3] and Kensaku Tamaki[2†]

[1]School of Creative Science and Engineering, Waseda University, 3-4-1 Okubo, Shinjuku-ku, Tokyo 169-8555, Japan
[2]Graduate School of Engineering, The University of Tokyo, 7-3-1 Hongo, Bunkyo-ku, Tokyo 113-8654, Japan
[3]Earthquake Research Institute, The University of Tokyo, 1-1-1, Yayoi, Bunkyo-ku, Tokyo 113-0032, Japan
[4]Global Center, Weathernews Inc., 1-3, Nakase, Mihama, Chiba, Chiba 261-0023, Japan
[5]Department of Geology, Faculty of Sciences, Niigata University, 8050, Ikarashi 2-no-cho, Nishi-ku, Niigata, Niigata 950-2181, Japan
[6]National Oceanography Centre, Southampton, University of Southampton, European Way, Southampton SO14 3ZH, U.K.
[7]Kochi Core Center, Japan Agency for Marine-Earth Science and Technology, 200 Monobe Otsu, Nankoku-shi, Kochi 783-8502, Japan
[8]Department of Science and Engineering, National Museum of Nature and Science, 4-1-1 Amakubo, Tsukuba, Ibaraki 305-0005, Japan

(*Received January 26, 2014; Accepted June 5, 2014*)

To ascertain factors controlling melt production along a typical distal, 'hotspot-interacting' mid-ocean ridge, we investigated the extent and distribution of both plume-related and plume-unrelated basalt from the central Indian ridge (CIR) between 15°S and 20°S. Comprehensive geochemical data of fresh-quenched volcanic glasses and basalts were used. Variation of Sr, Nd, and Pb isotopic compositions and Nb/Zr, Ba/Nb, and Ba/La content were interpreted by mixing of three melt end members: the Indian depleted MORB mantle derived melt; radiogenic and enriched melt derived from source mantle for Rodrigues Ridge and the intermediate series of Mauritius Island (RE2, radiogenic enriched component 2); and radiogenic but depleted melt derived from source mantle for Gasitao Ridge (RD, radiogenic depleted component). On the basis of quantitative mantle melting and melt mixing model, results show that sources for RE2 and RD are geochemically distinct from those of the Réunion plume (RE1, radiogenic enriched melt component 1). Moreover, the geochemical variation of MORB of 15°S to 20°S is unrelated to contamination of the upper mantle by the Réunion plume. These results suggest strongly that plume-unrelated heterogeneity is widespread throughout the upper mantle. The chemical characteristics of RE2 are remarkably pronounced in basalt from the central portion of ridge segment 16 around 18°S, suggesting substantial magma production. The influence of RE2 decreases along with decreasing magma production to the north, and is only slightly identifiable in basalt from the northern part of segment 18. Although the influence of RE2 decreases somewhat to the south, basalts with extreme RE2 signature were produced in the center of segment 15 around 19°S, where magma production is high. In contrast to RE2, the geochemical signature of RD in basalt is geographically limited to two localities: the south end of segment 18 and the center of segment 15. However, these observations reveal that both RE2 and RD contribute strongly to magma production on segment 15. Results show that melting of ancient recycled plate materials with a low melting point regulates voluminous magma production along the CIR.

Keywords: ridge-hotspot interaction, MORB geochemistry, crustal production, upper mantle, heterogeneity

Introduction

Upwelling of mantle plumes from deep in the Earth's interior is the most widely believed expression of mantle heat anomalies, along with upper mantle contamination by inclusion of recycled plate materials. Increased crust production by geochemically distinct magmas is a typical phenomenon along hotspot-influenced mid-ocean ridge (e.g., Ito *et al*., 2003; Schilling *et al*., 1982). The style of ridge-hotspot interaction are classifiable into three categories on the basis of the ridge-hotspot distance (Dyment *et al*., 2007). Along ridges directly over or in proximity to a hotspot, systematic geochemical variations can be determined corresponding to crustal volume, such as those seen on the Mid-Atlantic Ridge to near Iceland (e.g., Chauvel and Hémond, 2000; Murton *et al*., 2002; Blichert-Toft *et al*., 2005) or the Galapagos Spreading

*Corresponding author (e-mail: m-shikit@aoni.waseda.jp)

†Deceased.

Copyright © 2014 by The Geochemical Society of Japan.

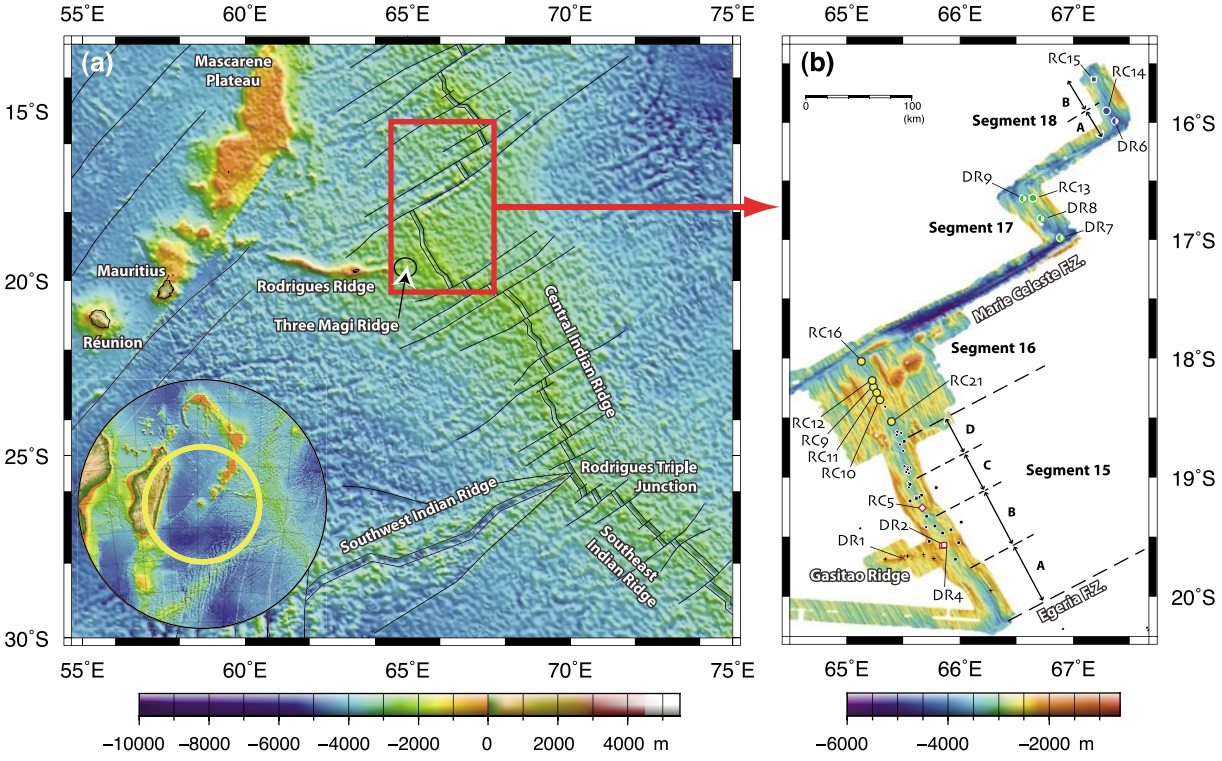

Fig. 1. Bathymetric maps around the Rodrigues segment (18–20°S, between the Marie Celeste and Egeria Fracture Zones) of the Central Indian Ridge and the Réunion hotspot. Bathymetric data are from ETOPO2 (NOAA National Geophysical Data Center; http://www.ngdc.noaa.gov/) for (a), and collected by a multi narrow beam system SeaBeam2120 during the KH06-04 cruise using the R/V Hakuho-maru for (b). Azimuthal projection of topography centered on the Réunion hotspot is also shown in (a). The yellow circle in (a) shows equidistance from the Piton de la Fournaise volcano of Réunion Island. From A to D, and A and B respectively represent sub segment numbers for segments 15 and 18.

Center closed to near the Galapagos hotspot (e.g., Schilling *et al*., 1982; Graham *et al*., 1993; Detrick *et al*., 2002; Cushman *et al*., 2004; Ingle *et al*., 2010; Colin *et al*., 2011). These geochemical variations are explained by mixing between enriched components included in the mantle plume and depleted upper mantle.

In contrast to these two localities, the style of interaction of the Central Indian Ridge (CIR) between 18°S and 20°S (Rodrigues segment) with the Réunion hotspot (Fig. 1), a typical case for distal ridge-hotspot interaction, is more complicated. The Rodrigues, Three Magi, and Gasitao Ridges (Fig. 1) show the topographic connection of the Réunion hotspot track with the CIR at 20°S, and is likely to resemble the Wolf-Darwin Lineament (Detrick *et al*., 2002) connecting the Galapagos Spreading Center and hotspot. Furthermore, northward enrichment of incompatible elements and radiogenic isotopes in mid-ocean ridge basalt (MORB) along the Rodrigues segment toward the Marie Celeste Fracture Zone (MCRZ) was observed. This enrichment suggests that an inflow of plume material channeled from the Réunion hotspot reaches CIR (Morgan, 1978; Mahoney *et al*., 1989; Murton *et al*., 2005).

Nauret *et al*. (2006) demonstrated that the geochemical anomaly on the Rodrigues segment cannot be explained simply by plume flow. They showed that neither a northward increase of Ba/Nb nor Pb isotope ratios corresponds to the Réunion hotspot. They reported that the geochemical trends for Gasitao Ridge and the southern part of the Rodrigues segment are explainable by mixing of the Réunion plume and depleted mantle. Moreover, they proposed that plume flow might reach as far as the segment around 20°S. However, they did not account for the slightly lower Ba/Nb ratio of Gasitao Ridge. They only classified one sample from the CIR axis as hotspot-influenced MORB. Therefore, only weak evidence exists for plume flow from the Réunion hotspot. The literature suggests that the Rodrigues, Three Magi, and Gasitao Ridges instead reflect the lithospheric tensional cracks through which melts from heterogeneous Indian Ocean mantle can pierce the lithosphere (e.g., Forsyth *et al*., 2006; Hirano *et al*., 2006; Dyment *et al*., 2007). Consequently, it might be true that there is no inflow taking place from the Réunion hotspot. Nauret *et al*. (2006) pro-

posed two hypotheses for northward enrichment: existence of metasomatized mantle during plate subduction, or some ancient recycling process in the upper mantle unrelated to the Réunion plume. However, characteristics of the enriched component remain undefined.

To resolve these issues, it is important to ascertain the extent of the distribution of the plume-related or plume-unrelated MORB crossing through the MCRZ. We produced a comprehensive geochemical dataset including major and trace element, water content, and Sr, Nd, and Pb isotopic composition for fresh quenched glasses and basalts along the CIR for 15–20°S. This dataset includes an area, between 15°S and 18°15′ S, for which no previous data have been available. Using this extensive dataset, we investigated which factors influence melt production along the hotspot-influenced CIR. Additionally, we infer a possible upper mantle structure that can explain the geochemical variations.

Geological Background, Field Observations, and Sample Collections

The Réunion hotspot formed a volcanic trail from Réunion Island (present location of the Réunion plume) to the Deccan continental flood basalt province (Fig. 1a). The submarine volcanic trail was split approximately 38 Ma by the CIR. Along-trail sampling conducted by drilling during the Ocean Drilling Program (ODP) Leg 115 (Backman *et al*., 1988) revealed that the trail was composed of tholeiite and alkaline basaltic lava (Baxter, 1990). The Rodrigues, Three Magi, and Gasitao Ridges (Fig. 1a) topographically connect the CIR with a volcanic trail formed on Oceanic crust younger than 36 Ma. The ridges comprise alkaline basaltic lava (Baxter *et al*., 1985; Murton *et al*., 2005; Nauret *et al*., 2006).

A high-resolution bathymetric investigation along the CIR (Fig. 1b) was conducted between 15°S and 20°S using a multiple narrow beam echosounder system (SeaBeam2120) with a sonic frequency of 20 kHz, and beam width of 1 degree during the KH06-04 cruise of the R/V Hakuho-maru. The CIR between 18°S and 20°S (Rodrigues segment) is separated into two segments, 15 (south) and 16 (north) (Fig. 1b). Segment 15 is further divided into four subsegments on the basis of morphological structure of axial valley, designated as 15A, 15B, 15C, and 15D from south to north. Segments 15 and 16 are characterized by shallow water depth relative to northern segments 17 and 18. Segment 18 is divided into two subsegments, designated as 18A and 18B from south to north. Gasitao Ridge, the eastern extension of Rodrigues ridge, reaches to the center of Segment 15B. Rock samples and fresh glasses were collected from the CIR axis and Gasitao Ridge using a dredge (labeled DR) and a rock corer (labeled RC). Sampling locations, which were arranged along segments 15, 16, 17, and 18, and Gasitao Ridge, and were selected on the basis of a high-resolution bathymetric investigation. A summary of sampling location is presented in Supplementary Table S1.

Analytical Methods

For major and trace element analyses of basaltic glasses, three fresh and fundamentally glassy pieces from each sample were hand-picked under a binocular microscope, mounted in epoxy, and polished with a diamond paste. To examine compositional heterogeneity, five spots were analyzed on three pieces from a sample. These analyses were averaged to provide major and trace element compositions for each sample. The major and trace element compositions were determined respectively using an electron probe microanalyzer (EPMA) and laser ablation inductively coupled plasma mass spectrometer (LA-ICP-MS), at the Earthquake Research Institute, the University of Tokyo. The EPMA instrument (JXA-8800; JEOL) had five wavelength-dispersive spectrometers. The EPMA analyses were conducted with acceleration voltage of 15 kV and beam current of 12 nA using a 5 μm diameter beam. Peak measuring times were 10 s for all major elements. Natural and synthetic mineral standards were used for the analyses. JEOL software using ZAF corrections was used. The LA-ICP-MS instrument (Plasma Quad 3; VG) was equipped with a laser ablation system of frequency-quintupled Nd-YAG laser (λ = 213 nm, UP-213; New Wave). The laser ablation system was used with a pulse repetition rate of 5 Hz, a preablation of 5 s, and an acquisition time of 60 s for each 65 μm diameter spot. During the analyses, 32 trace elements (Sc, V, Cr, Co, Ni, Rb, Sr, Y, Zr, Nb, Sb, Cs, Ba, rare-earth elements (REE), Hf, Ta, Pb, Th, and U) were monitored. A glass disc (SRM610; NIST) was used as a calibration standard, with preferred values taken from Pearce *et al*. (1997). As an internal standard, ^{44}Ca was used. The analytical procedures were described by Magnani *et al*. (2006). Relative standard deviations (RSD) of 15 repeat analyses for each basaltic glass sample were better than 5% in major elements, except for MnO and P_2O_5 and better than 20% in trace elements except for Cs and Sb on some samples.

Analyses of the volatile contents of volcanic glass were conducted using the FTIR Bench (Nicolet) controlled by 'OMNIC' data collection and processing software. Three spectra were recorded per glass chip. Site selections were made on the basis of constant color and appearance, with glass that is free of scratches, vesicles, surface contamination, crystals and other inhomogeneities. Total dissolved H_2O was measured using the intensity of the broad asymmetric band centered on 3550 cm^{-1}, which corresponds to the fundamental O–H stretching vibration (Nakamoto,

1997). Using the peak height calculation tool in the OMNIC spectral analysis software, a baseline was set, with peak height calculated for each spectrum. The molar absorptivity for total dissolved water is not strongly compositionally dependent for basaltic compositions. Therefore, a value of 63 ± 5 l/(mol cm) was used (Ferreira, 2006). Data for the three spectra were averaged. Then the standard deviations were calculated for the obtained concentrations.

For major and trace element analysis of whole rocks, initial subsamples of about 20 g of chips were separated from the quite fresh dredged rock samples. These subsamples were rinsed with distilled water for three days. Then they were washed ultrasonically in distilled water to remove seawater contamination. Removal was confirmed using silver nitrate solution ($AgNO_3$). The samples were pulverized using tungsten carbide mortar and an agate ball mill. The loss on ignition (LOI) was determined at 900°C (4 h). Major and minor elements were measured using an X-ray fluorescence (XRF) analyzer (RIX 3000; Rigaku Corp.) at the Niigata University according to the analytical methods described by Takahashi and Shuto (1997). Major elements were determined using fused glass discs. A mixture of 0.5 g of dried, powdered sample and 5.0 g of anhydrous lithium tetraborate ($Li_2B_4O_7$) was used for major element analysis without matrix correction because of the high dilution factor. Trace element contents were analyzed using ICP-MS (7500a; Agilent Technologies Inc.) at Niigata University, following the method described by Takazawa *et al*. (2003). Each 0.0500 g powdered rock sample was digested completely with 1 mL HNO_3 and 1.5 mL HF in a tightly sealed 7 mL Savillex® Teflon PFA screw-cap beaker, heated for 3 days on a hot plate at 120°C and subsequently evaporated for >6 h at 130°C. The residue was then dissolved with 6 mL HNO_3–HCl–HF ultrapure water (28:2:0.1:20) mixed acid with heating until perfectly dissolved. The solution was diluted to 50 g using ultrapure water including 1 mL internal standard solution (1 ppm each of In, Tm, Re, and Bi) in a 50 ml bottle. The solution was diluted further to 1:20,000 in mass, using mixed acid (120 mL previously used mixed acid is further diluted by 880 mL ultrapure water). Although ICP parameters were optimized, spectral overlap from oxides (MO^+) and hydroxides (MOH^+) of Ba and light REE on heavier REE ($^{137}Ba^{16}O^+$ on $^{153}Eu^+$; $^{141}Pr^{16}O^+$ on $^{157}Gd^+$; $^{143}Nd^{16}O^+$ on $^{159}Tb^+$; $^{147}Sm^{16}O^+$ on $^{163}Dy^+$; and $^{147}Sm^{16}O^1H^+$ on $^{165}Ho^+$) were found, which must be examined. Interference of $^{165}Ho^{16}O^+$ and $^{181}Ta^+$ was also inferred as a possibility. Corrections for interference were made by measuring two mixed standard solutions (2 ppb of Ba, Pr, Nd, and Sm, and 2 ppb of Eu, Dg, Tb, Dy, and Ho), and by calculating MO^+/M^+ and MOH^+/M^+ ratios. Trace element concentrations were calibrated using the reference values for BHVO-1 (U.S. Geological Survey (USGS)) of Eggins *et al*. (1997). Differences between our data and the accepted values for USGS standard W-2 (Eggins *et al*., 1997) were typically less than 5%.

The same rock powder analyzed for major and trace element analysis was also used for bulk rock Sr–Nd–Pb isotopic analysis. Some slightly altered basaltic glasses were leached using 2M HCl before Sr–Nd–Pb isotopic analysis. Total procedural blanks for Sr, Nd, and Pb were less than 100 pg. Sr and Nd isotope analyses were acquired using thermal ionization mass spectrometry (TIMS, Sector 54; VG) with seven Faraday collectors at the National Museum of Nature and Science, Japan. Approximately 0.1–0.2 g of powdered rock or glass samples were digested completely using 2 mL HNO_3, 5 mL $HClO_4$, and 5 mL HF in tightly sealed 30 mL Teflon PFA screw-cap beakers, heated for 18 h on a hot plate at 180°C, then evaporated for more than 5 h at 110°C. Finally, they were heated nearly to dryness at 180°C. The Sr and REE were separated using column separation with a cation exchange resin (AG50W-8X; Bio-Rad Laboratories Inc.). Then Nd was further isolated from the REE using Ln resin (Eichrom Technologies Inc.). The measured isotope ratios were normalized to $^{86}Sr/^{88}Sr = 0.1194$ and $^{146}Nd/^{144}Nd = 0.7219$. The average value for the NIST SRM-987 Sr standard was 0.710274 ± 0.000007, and for the JNdi-1 Nd standard of GSJ (Geological Survey of Japan) was 0.512111 ± 0.000004. The Pb isotopes were determined using multi-collector inductively coupled plasma mass spectrometry (MC-ICP-MS) NEPTUNE at the Center for Advanced Marine Core Research, Kochi University (Kochi Core Center). Approximately 0.08–0.13 g powdered rock or glass samples were digested with mixed acid (0.7 mL 8 M HBr and 0.7 mL 20 M HF) in a 7 mL PFA Teflon vial, heated at 130°C. After drying at 140°C, the sample was dissolved with 1 mL 0.5 M HBr and centrifuged. Pb was separated using anion exchange resin (AG 1-X8, 200–400 mesh, Br-form; Bio-Rad Laboratories Inc.) packed in a TFE Teflon column. An external Tl mass bias correction and standard bracketing method was used to improve the analytical precision. The analytical procedure follows the description presented by Tanimizu and Ishikawa (2006). The NIST SRM981 Pb standard was analyzed repeatedly between sequences of unknown sample analysis, giving the average values of $^{206}Pb/^{204}Pb = 16.9309 \pm 0.0017$, $^{207}Pb/^{204}Pb = 15.4844 \pm 0.0020$, and $^{208}Pb/^{204}Pb = 36.6754 \pm 0.0024$. These are similar to previous values determined using MC-ICP-MS with Tl-normalization, and are slightly lower than values determined by TIMS with ^{207}Pb–^{204}Pb double-spike (previous values are presented in Tanimizu and Ishikawa, 2006). Reproducibility was monitored by repeated analysis for the JB-2 GSJ standard, except for DR9A and DR6C with low Pb signal. The average values of the JB-2 GSJ stand-

ard are $^{206}Pb/^{204}Pb = 18.3213 \pm 0.0014$, $^{207}Pb/^{204}Pb = 15.5470 \pm 0.0018$, and $^{208}Pb/^{204}Pb = 38.2164 \pm 0.0020$.

All geochemical data are presented in Supplementary Table S2.

Results

Volcanic rocks from the CIR and Gasitao Ridge are range from 47.6–52.4 weight (wt.) percent in SiO_2. They show decreasing trends in MgO, and increasing trends in total alkali (Na_2O+K_2O) with increasing SiO_2 (Fig. 2). They also show decreasing trends in Al_2O_3 and CaO (or Al_2O_3/CaO), and increasing trends in TiO_2 and FeO* with decreasing MgO (Fig. 3). In Segment 15B (Fig. 1), basalts from RC5 and DR4 are similar in composition to those reported by Murton *et al*. (2005) and Nauret *et al*. (2006). Basalts from DR2 show higher Na_2O (Table S2) and total alkali (Fig. 2a) compositions, resembling some samples reported by Cordier *et al*. (2010). In segments 16, 17, and 18 (Fig. 1) almost all samples show similar compositions to those of previously reported basalts from Segment 15, except for basalts from DR6 at the southern end of Segment 18A, which have lower SiO_2 concentrations (48.14–48.55 wt.%), and basalts from Segment 17 (DR7, 8, and 9, and RC13), which have slightly higher total alkali compositions.

The trace element compositions of basalt from the CIR and Gasitao Ridge (Fig. 4) reveal additional evidence of geochemical variation from south to north (Fig. 1). Basalts from DR2 in Segment 15B are extremely enriched in highly incompatible elements such as Ba, U, and Nb when compared to representative samples from the Réunion hotspot. This difference corresponds to higher total alkali composition (Fig. 2a), similar to that of the Rodrigues samples (Baxter *et al*., 1985). In contrast, basalts from DR4 in Segment 15B show depleted trace element compositions resembling those of Gasitao Ridge (Nauret *et al*., 2006). Basalts from DR1 on Gasitao Ridge show slightly depleted compositions, in contrast to those reported previously (Nauret *et al*., 2006). They might indicate a more primitive (higher MgO and lower SiO_2) composition (Fig. 2). Basalts from RC5 in Segment 15B show lower amounts of highly incompatible elements than in primitive mantle (McDonough and Sun, 1995). These samples display features in major elements that resemble those of basalts reported previously from Segment 15 (Murton *et al*., 2005; Nauret *et al*., 2006). Basalts from Segment 16, and DR7, DR9, and RC13 on Segment 17 show higher amounts of highly incompatible elements. Basalts from DR8 in Segment 17, and RC14 and 15 in Segment 18 show somewhat lower amounts of highly incompatible elements, similar to basalts from RC5 in Segment 15B. Furthermore, basalts from DR6 in Segment 18 show depleted trace element compositions resembling

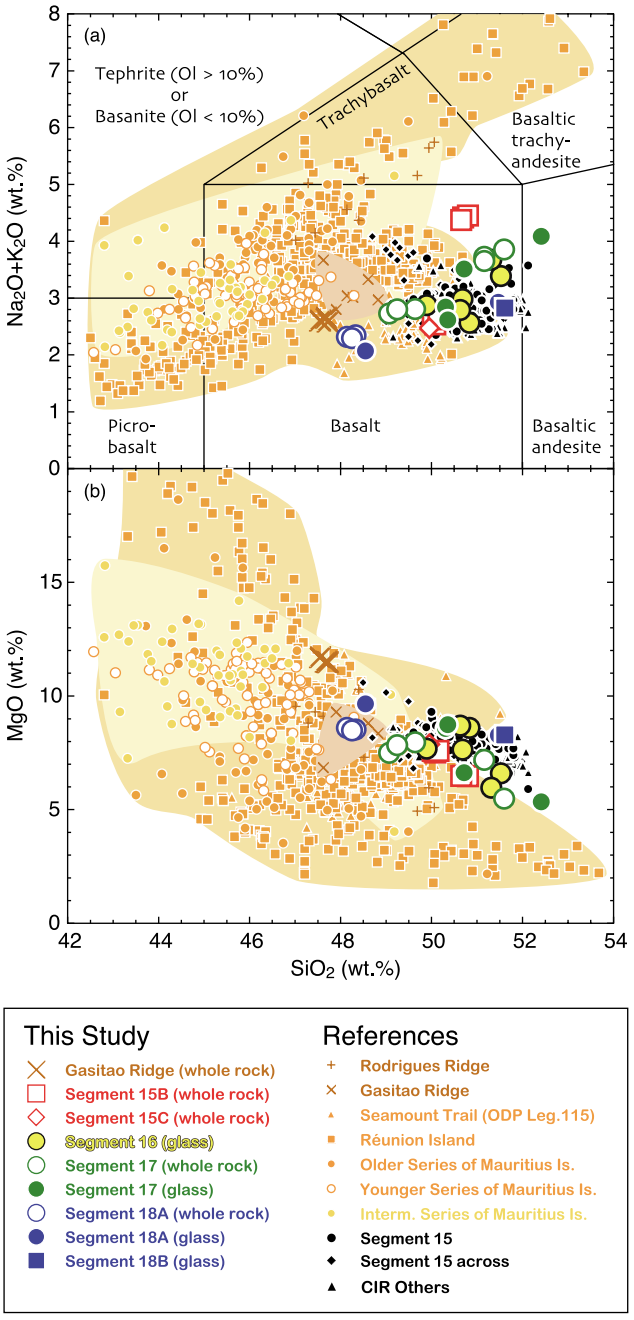

Fig. 2. Total alkalis (a) and MgO (b) vs. SiO_2 diagram for basalts from Gasitao Ridge and the Central Indian Ridge for 15°S through 20°S. Discrimination boundaries in (a) after Le Bas et al. (1986). Previously reported CIR data (CIR others), along axis data from Segment 15 (Segment 15), and across axis data from Segment 15 (Segment 15 across) are respectively referred from the PetDB database, from Murton et al. (2005), Nauret et al. (2006), and Cordier et al. (2010). Details of data compilation for basalts from Réunion Island (Réunion), older and intermediate series of the Mauritius Island (Mauritius Old and Mauritius Intermediate), seamount trail from the Réunion Island along hotspot track (Seamount Trail), and Rodrigues, and Gasitao ridges are described in Supplementary Materials.

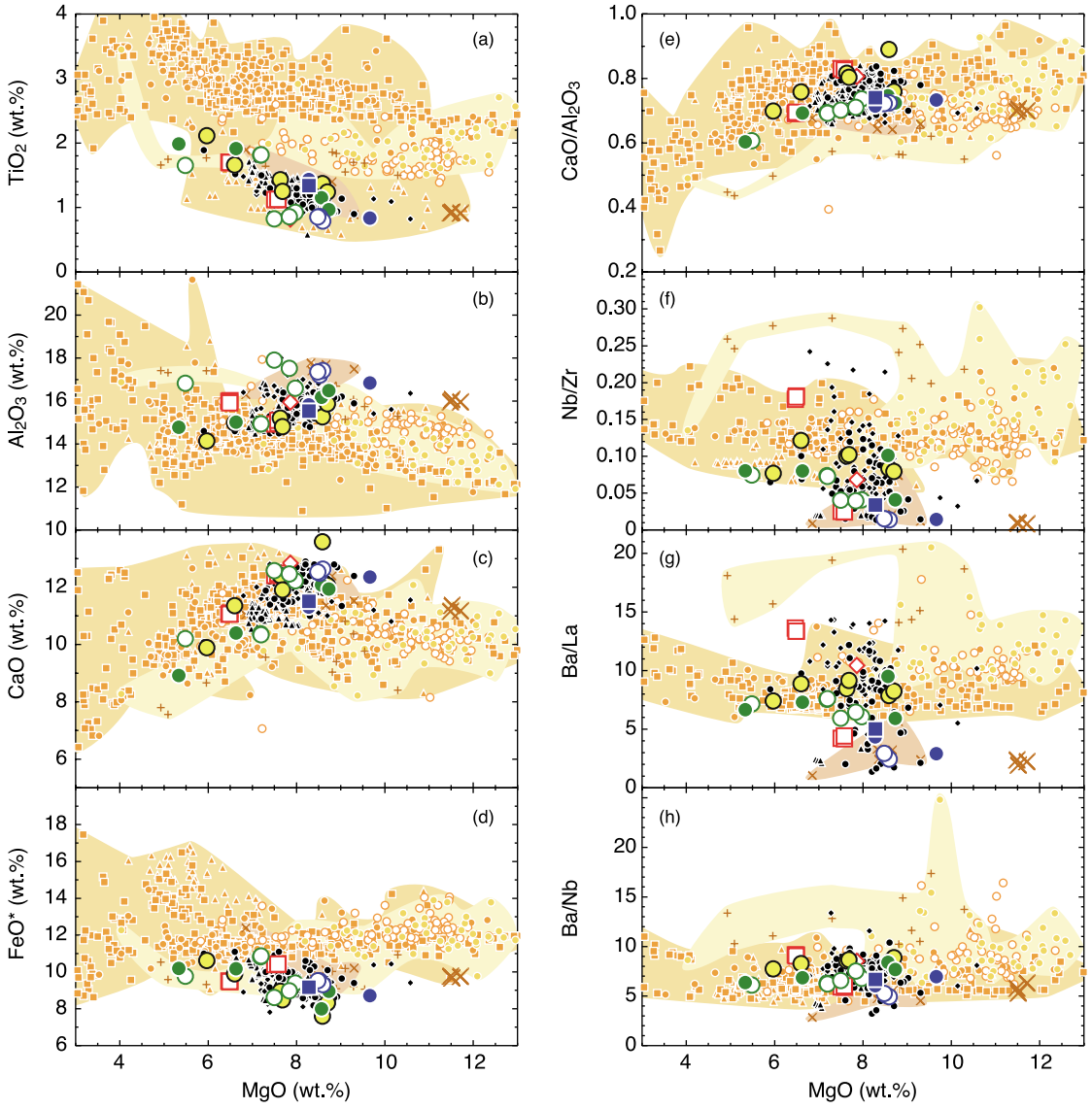

Fig. 3. Diagrams showing variations of TiO_2 (a), Al_2O_3 (b), CaO (c), FeO (d), CaO/Al_2O_3 (e), Nb/Zr (f), Ba/La (g), and Ba/Nb (h) against MgO of basalts from Gasitao Ridge and the Central Indian Ridge for 15°S through 20°S. Symbols and references for other compiled data as in Fig. 2.*

those of Gasitao Ridge (Nauret *et al.*, 2006), DR1, and DR4. These differences of constituent highly incompatible elements of basalts are represented as variation of Nb/Zr, Ba/La, and Ba/Nb for basalts having similar MgO composition (Fig. 3).

The isotopic composition of basalts from the CIR (Fig. 5) shows that relatively enriched compositions are observed in segments 15 and 16 (0.703181–0.703586 on $^{87}Sr/^{86}Sr$, 0.512926–0.513017 on $^{143}Nd/^{144}Nd$, 18.3467–18.8353 on $^{206}Pb/^{204}Pb$, 15.5036–15.5582 on $^{207}Pb/^{204}Pb$, and 38.2416–38.8958 on $^{208}Pb/^{209}Pb$), gradually becoming more depleted northward through segments 17 and 18 (0.702922–0.703263 on $^{87}Sr/^{86}Sr$, 0.512999–0.513103 on $^{143}Nd/^{144}Nd$, 18.0575–18.3736 on $^{206}Pb/^{204}Pb$, 15.4684–15.5339 on $^{207}Pb/^{204}Pb$, and 37.9033–38.3592 on $^{208}Pb/^{209}Pb$). The most radiogenic samples were collected from DR4 in the center of Segment 15B. This trend conforms to previous observations reported by Mahoney *et al.* (1989) and Nauret *et al.* (2006). Variation of isotopic composition (Fig. 5) shows that relatively radiogenic basalts from segments 15 and 16 of the CIR have similar composition to basalts from Rodrigues Ridge and the Intermediate series of the Mauritius Island showing lower $^{87}Sr/^{86}Sr$, and slightly higher $^{143}Nd/^{144}Nd$ and lower $^{207}Pb/^{204}Pb$ and $^{208}Pb/^{209}Pb$ (Baxter *et al.*, 1985; Sheth *et al.*, 2003; Nohda *et al.*, 2005; Moore *et al.*, 2011), rather

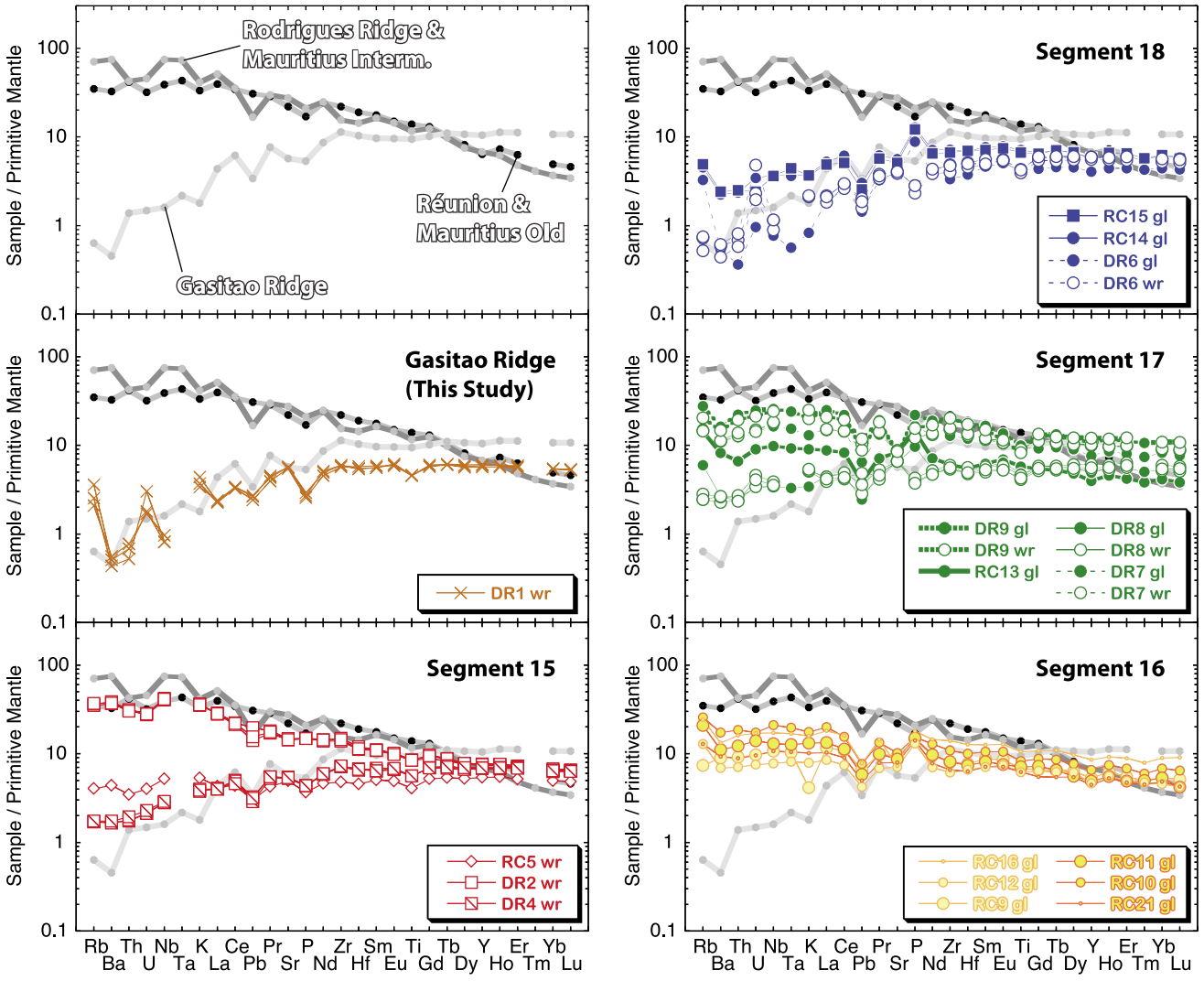

Fig. 4. Trace element concentrations normalized to primitive mantle (McDonough and Sun, 1995) for basalts from Gasitao Ridge and the Central Indian Ridge for 15°S through 20°S. Representative data of basalt from Réunion Island and Older series of Mauritius Island (sample M12), Rodrigues Ridge and the Intermediate series of Mauritius Island (sample B5), and Gasitao Ridge (sample DR08-1) are from Moore et al. (2011), Sheth et al. (2003), and Nauret et al. (2006), respectively.

than basalts from Réunion Island, the Older series of Mauritius Island, and the seamount trail of the Réunion hotspot (e.g., Albarède and Tamagnan, 1988; Fisk *et al.*, 1988; Mahoney *et al.*, 1989; Baxter, 1990; White *et al.*, 1990; Albarède *et al.*, 1997; Fretzdorff and Haase, 2002; Sheth *et al.*, 2003; Nohda *et al.*, 2005; Paul *et al.*, 2005; Moore *et al.*, 2011) as typical compositions of the Réunion plume (see in Supplementary Materials for detail on data compilation). In contrast, less radiogenic basalts from segments 17 and 18 show lower $^{143}Nd/^{144}Nd$ and higher $^{87}Sr/^{86}Sr$ for given $^{206}Pb/^{204}Pb$, rather than depleted MORB mantle (DMM: Workman and Hart, 2005). These observations are also shown by three-dimensional variation diagrams for Sr, Nd, and Pb isotopic space (see Supplementary Fig. S4).

The basalt from Gasitao Ridge has a radiogenic Sr and Pb isotopic composition (Fig. 5), despite having a depleted trace element composition (Fig. 4). These results are also consistent with observations for Gasitao Ridge reported by Nauret *et al.* (2006).

Discussion

Geochemical variation of MORB from the Rodrigues and neighboring segments along the CIR

Important correspondence between isotopic and trace element compositions of MORB from the Rodrigues segment (Segment 15 and 16) is that the basalts having ra-

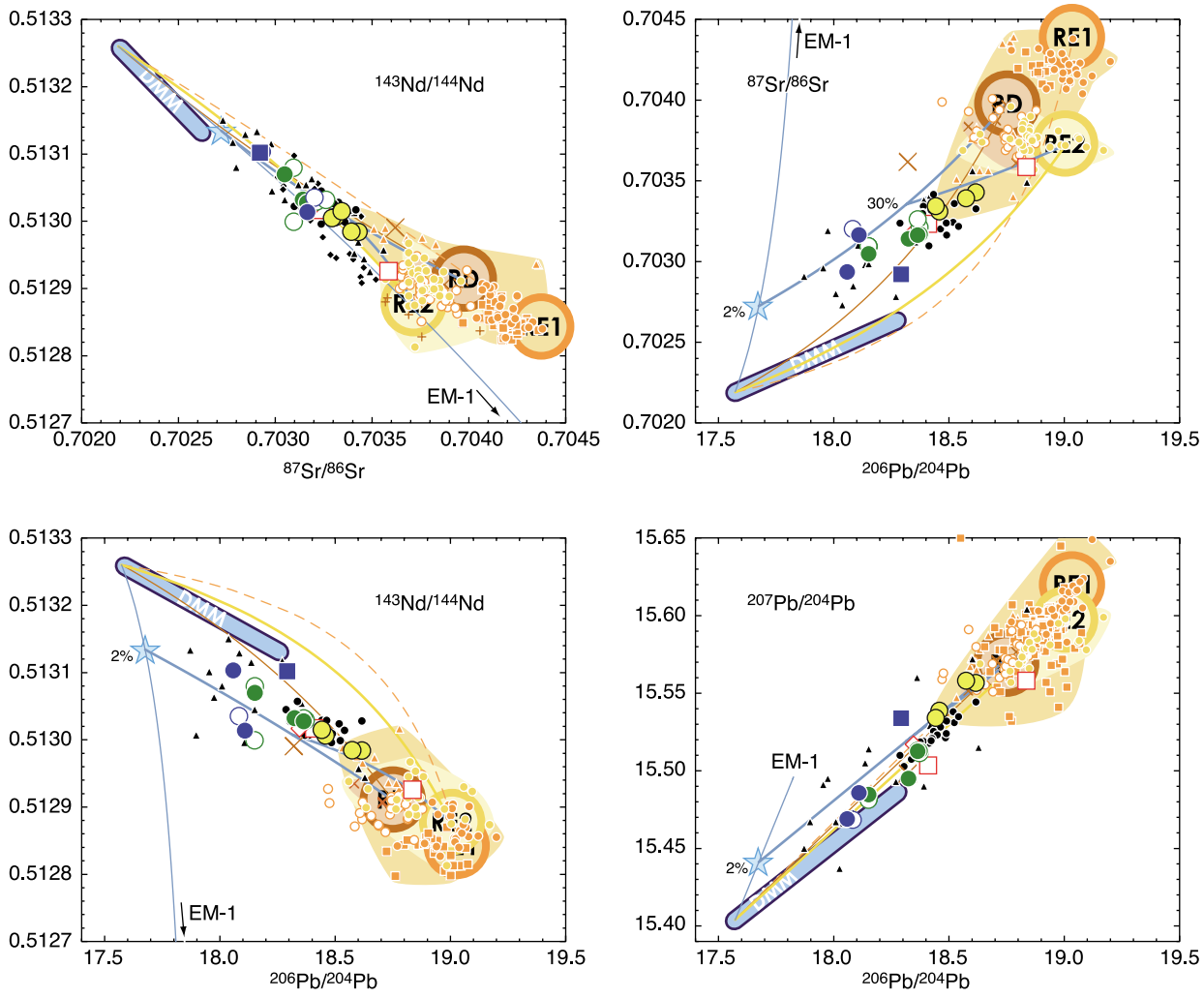

Fig. 5. Sr–Nd–Pb isotopic variations of basalts from Gasitao Ridge and the Central Indian Ridge for 15°S through 20°S. Symbols and references for other compiled data as in Fig. 2. RE1 (orange circle), RE2 (yellow circle), and RD (brown circle) respectively show radiogenic-melt end members derived from the Réunion plume, the source of the Intermediate series of Mauritius Island and Rodrigues ridge, and the source of Gasitao Ridge. Variation range of D-DMM and averaged DMM (labeled "DMM") are from Workman and Hart (2005). The orange dashed line and yellow and brown lines respectively represent results of binary mixing between D-DMM-derived melt and RE1, RE2, and RD. The light blue lines represent results of binary mixing between D-DMM-derived melt and EM-1 melt, and ternary mixing D-DMM-derived melt, RD, and EM-1 melt. 1% and 30% respectively denote amounts of EM-1 melt and RD. Details of definitions and compositions of radiogenic-melt end members, D-DMM-derived melt, and EM-1 melt are listed in Supplementary Materials.

diogenic isotopic composition (Fig. 5) show high Nb/Zr, Ba/Nb, and Ba/La (Figs. 3, 4, and 6). Then, they have similar isotopic and trace element compositional features to basalts from Rodrigues Ridge and the Intermediate series of the Mauritius Island, not similar to basalts from Réunion Island (Fig. 6). In contrast, it is also presented in Figs. 3, 4, and 6 that some samples from Segment 15, 17, and 18 show very low Nb/Zr, Ba/Nb, and Ba/La, and these compositions resembling those of basalts from Gasitao Ridge. As described in previous section, wide variation of Nb/Zr, Ba/Nb, and Ba/La is observed on basalts having similar MgO composition (Fig. 3). Therefore, such variation on Nb/Zr, Ba/Nb, and Ba/La of CIR basalts cannot be explained by fractional crystallization of single primary magma. Furthermore, we note that a characteristic isotopic composition of less radiogenic basalts, that is lower $^{143}Nd/^{144}Nd$ and higher $^{87}Sr/^{86}Sr$ for given $^{206}Pb/^{204}Pb$ than DMM, should be considered. On the basis of these observations, we propose that several kinds of melt components contribute to geochemical variation and magma genesis along CIR segments 15 through 18.

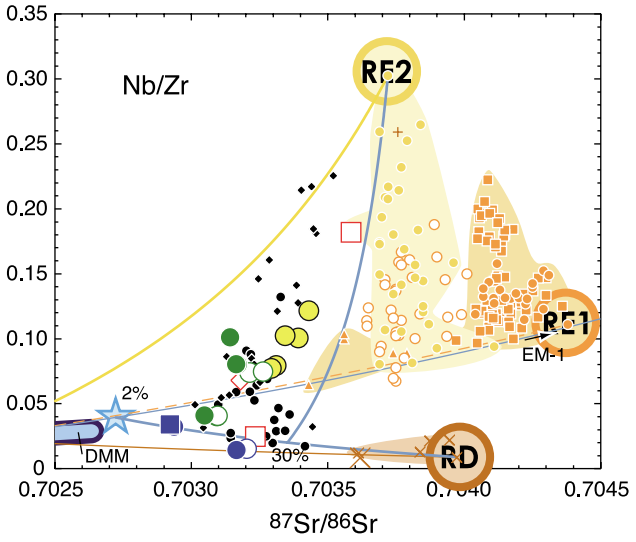

Fig. 6. Nb/Zr vs. $^{87}Sr/^{86}Sr$ variation diagram indicating that the geochemistry of basalt from Gasitao Ridge and the Central Indian Ridge, is enhanced by Depleted MORB Mantle (DMM), enriched melt components of two kinds (RE2 and RD) unrelated to the Réunion plume (RE1), and some EM-1 melt. Symbols and references for other compiled data as in Fig. 2. Mixing results are denoted by yellow, brown, and light blue lines and the orange dash line as in Fig. 5. The variation range of D-DMM and averaged DMM (labeled "DMM") are from Workman and Hart (2005).

To verify these qualitative considerations, we conducted numerical mixing calculations for Sr, Nd, and Pb isotopes and Nb/Zr, Ba/Nb, and Ba/La ratios (Figs. 5, 6, and Supplementary Figs. S4, S5, S6, and S7). For the mixing model, we define four melt end members (Table 1) on the basis of previous observations as follows. The geochemistry of basalts from Réunion Island and the Older series of Mauritius Island is characterized by a specific enriched melt composition, showing the most-radiogenic Sr isotopic compositions, and slightly high Nb/Zr, La/Nb, and Ba/Nb (Fig. 3, and Supplementary Figs. S1, S2, and S3). Hereinafter, we call this end member 'Radiogenic Enriched Component 1' (RE1). And we defined sample M12 (Moore *et al.*, 2011), with the highest $^{87}Sr/^{86}Sr$ (=0.70438) as a representative sample for RE1 (Table 1). In contrast, basalts from the Intermediate series of Mauritius Island show less-radiogenic Sr isotopic compositions, as reported by Sheth *et al.* (2003), Nohda *et al.* (2005), and Moore *et al.* (2011). They therefore show a separate trend in $^{87}Sr/^{86}Sr$ and $^{143}Nd/^{144}Nd$ or $^{206}Pb/^{204}Pb$ variation diagrams (Figs. 5 and S4). This component is characteristic of the geochemistry of basalts from Rodrigues Ridge (Baxter *et al.*, 1985). Furthermore, basalts from Rodrigues Ridge and the Intermediate Series of Mauritius Island higher Nb/Zr, Ba/La, and Ba/Nb than the Réunion hotspot (Figs. 3, S1, S2, and S3). We defined sample B5 (Sheth *et al.*, 2003; Table 1) with the highest Nb/Zr (0.302) as the representative sample for the radiogenic-melt end member 'Radiogenic Enriched Component 2' (RE2). Gasitao Ridge (Nauret *et al.*, 2006) forms the third group, having extremely low Nb/Zr ratios in contrast to RE1 and RE2, but radiogenic isotopic composition. We base this end member on the composition of the representative sample DR08-1 (Nauret *et al.*, 2006; Table 1) with the highest $^{87}Sr/^{86}Sr$ (=0.703973) among the extremely low Nb/Zr basalts from Gasitao Ridge. Hereinafter, we call it the 'Radiogenic Depleted Component' (RD). The Indian Ocean MORB is known to be distinct from those of the Pacific. Fundamentally, it is more "EM-1-like" (e.g., Dupré and Allègre, 1983). Then, the Indian depleted upper mantle can be mixture of DMM and EM-1. Such plume-unrelated heterogeneity of EM-1 in the upper mantle is expected to have a small-scale (Machida *et al.*, 2009). Therefore, we also define the Indian-DMM-derived melt component on the basis of mixing of D-DMM-derived melt and a small amount (about 2%) of EM-1 melt (Table 1, and see details in Supplementary Materials).

Variation diagrams of isotopic composition (Fig. 5) show that basalts from the CIR plot a considerabe distance from the binary mixing line of D-DMM-derived melt and RE1. Furthermore, CIR basalts seem to contain not RE1 but RE2, especially shown in the $^{143}Nd/^{144}Nd$ and $^{87}Sr/^{86}Sr$ or $^{206}Pb/^{204}Pb$ and $^{87}Sr/^{86}Sr$ plots. These observations suggest that RE1 did not contribute to the production of magma along the CIR. However, the low $^{206}Pb/^{204}Pb$ and high $^{87}Sr/^{86}Sr$ compositional trend cannot be explained by simple binary mixing of D-DMM-derived melt and RE2. Such isotopic compositions would, however, be explained by the Indian-DMM-derived melt with the additional contribution from EM-1. High Nb/Zr, Ba/Nb, and Ba/La trend of the CIR basalts (Fig. 6, and Supplementary Materials) are also explained by contribution of RE2 rather than RE1. Furthermore, low Nb/Zr, Ba/Nb, and Ba/La samples are expected to be explained by a contribution from RD. Therefore, if we assume ternary mixing of Indian-DMM-derived melt, RE2, and RD, then the various Sr, Nd, and Pb isotopes and Nb/Zr, Ba/Nb, and Ba/La ratios of all data, including the previously reported data from Segment 15 (Murton *et al.* (2005) and Nauret *et al.* (2006) for 'along axis', and Cordier *et al.* (2010) for 'across axis'), are explained consistently (Figs. 5 and 6). Our mixing model shows that the major radiogenic (or enriched) melt components are RE2 and RD.

Nature of radiogenic melt components for CIR basalts

Isotopic compositions between the Réunion plume (RE1) and Rodrigues Ridge (RE2) (Figs. 5 and S4) are independently, although slightly, different. Basalts from

Table 1. Compositions for representative samples for the Réunion hotspot and neighboring volcanic edifices, and melt end members used in the mixing model

End members	RE1	RE2	RD	D-DMM melt	EM-1 melt
References	Moore *et al.* (2011)	Sheth *et al.* (2003)	Nauret *et al.* (2006)	Workman and Hart (2005), Salters and Stracke (2004)*, This study**	Jackson and Dasgupta (2008)
Volcanoes	Mauritius Old	Mauritius Interm.	Gasitao		Pitcairn
Sample ID	M12	B5	DR08-1		
SiO_2 (wt.%)	45.34	44.13	47.62		49.03
MgO (wt.%)	7.33	10.64	6.85		10.73
Na_2O+K_2O (wt.%)	3.71	4.24	3.67		4.16
LOI (wt.%)	1.15	0.64			
Sr (ppm)	437.8	545	113	38	518
Zr (ppm)	230.8	162	119	25	242
Nb (ppm)	25.6	49	1.05	0.57	29.83
Ba (ppm)	213.5	491	3	2	256
La (ppm)	25.55	33.2	2.82	0.87	28.39
Nd (ppm)	30.54	30.9	10.76	2.93	32.41
Pb (ppm)	4.61	2.5	0.51	0.09	2.99
$^{87}Sr/^{86}Sr$	0.70438	0.70372	0.703973	0.70219	0.704642
$^{143}Nd/^{144}Nd$	0.51284	0.512875	0.512911	0.51326	0.512577
$^{206}Pb/^{204}Pb$	19.0374	19.004	18.7465	17.573	17.826
$^{207}Pb/^{204}Pb$	15.6192	15.598	15.5716	15.404	15.496
$^{208}Pb/^{204}Pb$	39.1765	39.133	38.7042	37.057	38.855

**$^{208}Pb/^{204}Pb$ of DMM proposed by Salters and Stracke (2004) is substitute for that of D-DMM.*

***Trace element compositions of D-DMM-derived melt end member (D-DMM melt) are calculated assuming 15% batch melting of spinel peridotite. Melting parameters are from Supplementary Table S4.*

Rodrigues Ridge and the Intermediate series of Mauritius Island (RE2) show lower $^{87}Sr/^{86}Sr$ and slightly higher $^{143}Nd/^{144}Nd$ than that of the Réunion lavas (RE1). On the basis of such isotopic difference, it is expected that they could be derived from source having different trace element composition each other. This idea is supported by observations that some basalts from Rodrigues Ridge and the Intermediate series of Mauritius Island show high Nb/Zr, Ba/Nb, and Ba/La values, as presented in Figs. 3 and 6. During mantle melting, however, the Nb/Zr, Ba/Nb, and Ba/La ratios of magma will change according to the degree of partial melting because of differences of these partition coefficients for mantle lithology (e.g., Kelemen *et al*., 2003). Total alkali composition, as an index of the degree of partial melting, shows a clear positive correlation with Nb/Zr (Fig. 7a). Therefore, the difference in the degree of partial melting contributes to the observed Nb/Zr variation. However, we see that $^{87}Sr/^{86}Sr$ and Nb/Zr values of lavas from Rodrigues Ridge and the Intermediate series of Mauritius Island are clearly lower and higher, respectively, than that of lavas from Réunion Island, even at the same total alkali composition (Figs. 7a and 7b). Then, it is possible that not only the degree of melting, but Nb/Zr variations in the source material also contribute to the variation in Nb/Zr of lavas among those of Réunion Island, Rodrigues Ridge and the Intermediate series of Mauritius Island. Furthermore, Hanyu *et al*. (2001) demonstrated that the Intermediate and Younger series of Mauritius and Rodrigues Ridge have significantly lower (MORB-like) $^{3}He/^{4}He$ than the samples from Réunion and the Older Series of Mauritius. On the basis of these considerations, the involvement of a distinct enriched component contributing the genesis of Rodrigues Ridge and the Intermediate series of Mauritius Island is required.

We examine the difference in trace element compositions of source for each three radiogenic-melt end members (RE1, RE2, and RD) using a numerical non-modal batch melting model, as presented below (see Supplementary Materials for detailed modeling parameters). Garnet or spinel peridotite was assumed respectively for RE1 and RE2 or RD. The mafic lava showing slightly high Nb/Zr (0.111) (sample M12 from the Older series of Mauritius Island, Moore *et al*., 2011) is selected as representative of lava from the Réunion plume (RE1) because it is an endmember showing the highest $^{87}Sr/^{86}Sr$ (0.70438) (Table 1). We calculate source compositions of sample M12 assuming 10% or 25% melting. These sources respectively produce melts showing Nb/Zr = 0.157 or 0.214 results from 5% melting (Fig. 7c). In the latter case (25% melting), the Nb/Zr value matches the highest actual Réunion lava (Fig. 7b), but it is lower than the highest value of Rodrigues Ridge or the Intermediate series of Mauritius lava. However, the total alkali composition of sample M12 (3.71 wt.%) is best explained by about 10% mantle melting on the basis of melting experiments (e.g., Kushiro,

1994). Therefore, our modeling clearly illustrates that the Réunion source cannot produce the high Nb/Zr Intermediate of Mauritius (or Rodrigues) lava. The composition of the source for the Intermediate series of Mauritius is calculated from the mafic representative lava showing the highest Nb/Zr (0.302) (sample B5, Sheth *et al.*, 2003; Table 1) assuming 5% melting (Fig. 7c). Melting of this source produces higher Nb/Zr values than that of the representative lava of the Réunion plume (sample M12, Moore *et al.*, 2011, Nb/Zr = 0.111). Furthermore, considering results of melting experiments (e.g., Kushiro, 1994), 5% melting of the source would be an underestimation for sample B5, having 4.24 wt.% total alkalis. If we assume a higher degree of melting for the source calculation, then the Nb/Zr value of the produced lava will be even higher. Therefore, it is also true that we cannot produce the Réunion lava from the Rodrigues source. The same discussion is applicable to modeling of Ba/Nb or Ba/La (see Supplementary Fig. S8). Therefore, the results of our melting model indicate that the difference in the degree of partial melting alone cannot explain the extremely wide Nb/Zr (Ba/Nb and Ba/La) variations observed in the region. We propose that RE2 contributing genesis of Rodrigues Ridge and the Intermediate series of Mauritius Island was produced by melting of an independent source having higher Nb/Zr, Ba/Nb, and Ba/La, and lower $^{87}Sr/^{86}Sr$ than those of the Réunion plume (RE1).

The geochemistry of basalts from Gasitao Ridge was interpreted by Nauret *et al.* (2006) as evidence for the flow channeled from the Réunion hotspot. Nauret *et al.*

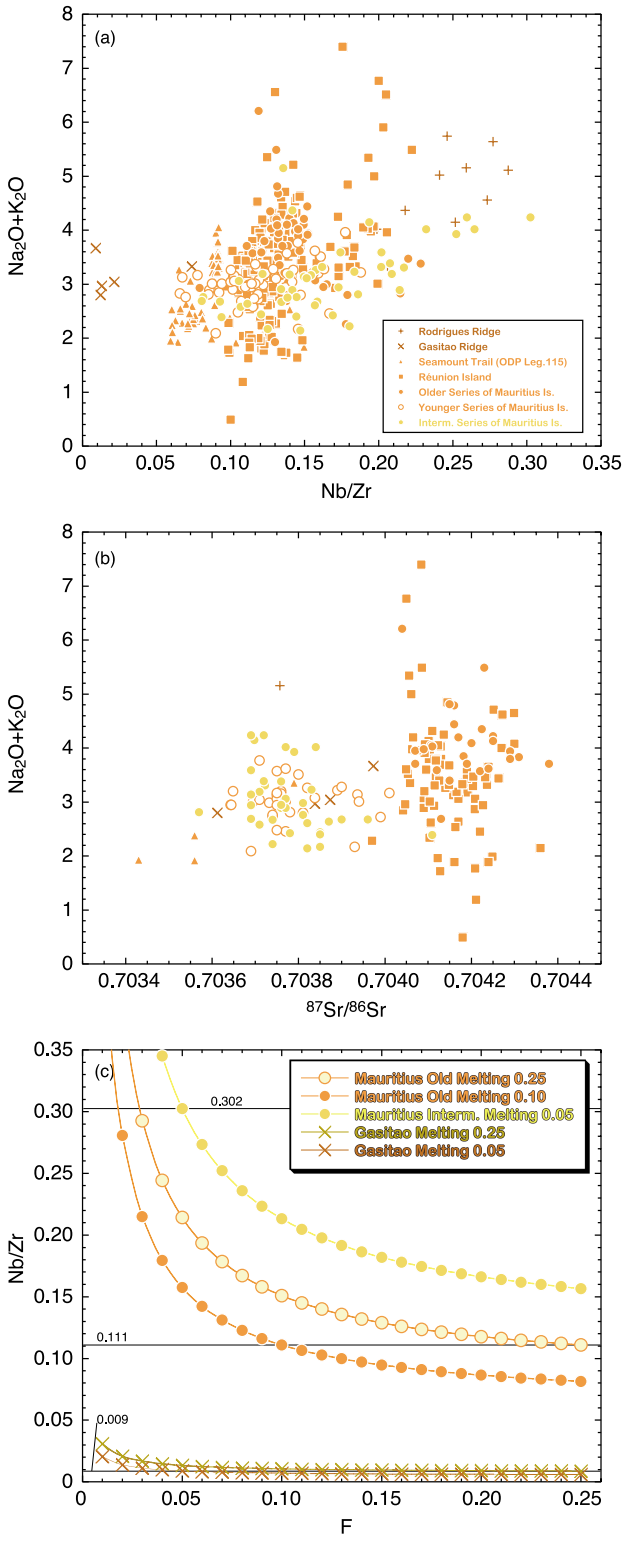

Fig. 7.

Fig. 7. Diagrams of total alkali (Na_2O+K_2O) vs. (a) Nb/Zr and (b) $^{87}Sr/^{86}Sr$ of basalts from Réunion Island (Réunion), Older and Intermediate series of the Mauritius Island (Mauritius Old and Mauritius Intermediate), seamount trail from Réunion Island along-hotspot track (Seamount Trail), and Rodrigues, and Gasitao ridges, and (c) Nb/Zr vs. degree of partial melting (F) comparing results of batch melting model. Black lines show Nb/Zr values for representative RE1 basalt from Réunion Island and Older series of Mauritius Island (sample M12, Moore et al., 2011, Nb/Zr = 0.111), RE2 basalt from Rodrigues Ridge and the Intermediate series of the Mauritius Island (sample B5, Sheth et al., 2003, Nb/Zr = 0.302), and RD basalt from Gasitao Ridge (sample DR08-1, Nauret et al., 2006, Nb/Zr = 0.009), respectively. The composition of the source for each melting model was calculated from the composition of representative RE1 basalt assuming 25% or 10% melting (Mauritius Old Melting 0.25 or 0.10), the composition of representative RE2 basalt assuming 5% melting (Mauritius Interm. Melting 0.05), and the composition of representative RD basalt assuming 25% or 5% (Gasitao Melting 0.25 or 0.05). Parameters for a melting model and modeling assumptions are presented in Supplementary Materials.

(2006) also considered one sample from the CIR (named DR10-1) with similar geochemistry to that of Gasitao Ridge as evidence indicating that mantle flow from the Réunion plume reaches the CIR. $^{143}Nd/^{144}Nd$ vs. $^{87}Sr/^{86}Sr$ or Ba/Nb vs. $^{206}Pb/^{204}Pb$ variations (Fig. 5, and figure 6 in Nauret *et al*. (2006)) are likely to support their interpretation. However, Fig. 6 shows clearly that basalts from Gasitao Ridge have extremely low Nb/Zr ratios, rather than RE1-like and RE2-like ratios. These differences are also observed on the primitive-mantle-normalized multi-element plot (Fig. 4). As shown in our melting model (Fig. 7c, see Supplementary Materials for additional details), even if the degree of melting is changed drastically, it is impossible to produce the Réunion and Rodrigues (or the Intermediate series of Mauritius) lava from the Gasitao source because the Nb/Zr, Ba/Nb, and Ba/La of Gasitao Ridge lava is too low. The extreme Nb/Zr, Ba/Nb, and Ba/La differences observed between Gasitao and the other volcanic edifices cannot result from the melting of a common mantle source. Therefore, the geochemistry of Gasitao Ridge indicates the existence of other distinct components in the mantle source.

RE1 contributes commonly the magma genesis during the long-lived Réunion hotspot activities from Réunion Island to the Deccan continental flood basalt province (Albarède and Tamagnan, 1988; Fisk *et al*., 1988; Mahoney *et al*., 1989; Baxter, 1990; White *et al*., 1990; Peng and Mahoney, 1995; Albarède *et al*., 1997; Fretzdorff and Haase, 2002; Sheth *et al*., 2003; Nohda *et al*., 2005; Paul *et al*., 2005; Moore *et al*., 2011), as shown also by our data compilation. In contrast to RE1, RE2 was only visible on the Intermediate series of Mauritius Island during hotspot activities (Sheth *et al*., 2003; Nohda *et al*., 2005; and Moore *et al*., 2011). And, RD is not observed along the Réunion hotspot track. On the other hand, our results show that the sources for RE2 and RD contribute largely to magma genesis along the CIR, indicating existence of radiogenic components (distinct from RE1) in upper mantle beneath the CIR. If the Réunion plume interact with CIR, the source of RE1 as a major radiogenic constituent of the plume must be distributed widely and then contribute magma genesis along CIR rather than sources for RE2 and RD. However, RE1 is not necessary for magma genesis of the CIR (and Rodrigues Ridge) as shown clearly by our mixing model. Therefore, a reasonable consideration is that sources for RE2 and RD are not constituents of the Réunion plume, and are plume-unrelated heterogeneity of the Indian upper mantle which regionally distribute around the CIR. Helium isotope ratios for the Rodrigues, Three Magi, and Gasitao Ridges, and the northern part of Segment 15 are somewhat high (Füri *et al*., 2011), suggesting a connection with the Réunion hotspot. To explain the inconsistent chemical features between He (noble gases) and other solid elements, Füri *et al*. (2011) proposed progressive depletion by melting en route to the CIR. However, such a process would result in "degassed" material. Therefore we should not expect to detect such a high He isotopic ratio. In fact, it is necessary to consider the higher diffusion rates of noble gases than those of most other incompatible elements (e.g., Sr, Nd, and Pb) because of their chemical inertness (e.g., Sneeringer *et al*., 1984; Cherniak, 1998; Trull and Kurz, 1993; Van Orman *et al*., 2001, Parman *et al*., 2009). Consequently, at a long distance from the plume, the diffusion behavior of noble gases and other elements becomes decoupled. It is an oversimplification to say that noble gases (or volatiles) diffuse from the hotspot, pollute the heterogeneous mantle, and reach the CIR. Especially in the case of Gasitao Ridge because the source was originally depleted and degassed, containing almost no noble gases, Helium isotope ratios of the plume origin are expected to be visible even on addition of a small plume component. Gasitao Ridge shows no evidence for plume flow from the Réunion hotspot. We conclude that the Rodrigues (or the Intermediate series of Mauritius) and Gasitao Ridge source components originate from plume-unrelated heterogeneity existing in the Indian Ocean mantle domain. The RE2 source is expected to be entrained in the ascending Réunion plume, and to contribute to the volcanic activity of the Réunion hotspot, especially for the Intermediate Series of Mauritius. This scenario is consistent with the model proposed earlier by Nohda *et al*. (2005) and by Moore *et al*. (2011) as one possibility for the origin of the Intermediate Series of Mauritius. Finally, results of our investigation indicate strongly that only plume-unrelated mantle heterogeneity alone is responsible for magma genesis and geochemical variation along the CIR at 15–20°S.

How does Plume-unrelated heterogeneity contribute to magma production along the Central Indian Ridge?

Results show that the geochemistry of the CIR is explainable by melting of DMM (with small-scale EM-1 heterogeneity) and two major regional radiogenic mantle components unrelated to the Réunion plume (the source for RE2 and RD). To investigate how these two components contribute to melt production along the CIR, we specifically examine along-axis variation of Nb/Zr and $^{87}Sr/^{86}Sr$ (Fig. 8) because these geochemical tracers are suitable for identification of these components. Additionally, we examine the relation between magma chemistry and productivity (crustal volume) inferred from the water depth and the morphology of volcanic edifices.

Along-axis geochemical variation on the Central Indian Ridge The chemical characteristics of RE2 appear remarkably pronounced in basalt from the central portion of Segment 16. Substantial magma production here is inferred on the basis of results of shallow ridge bathymetry

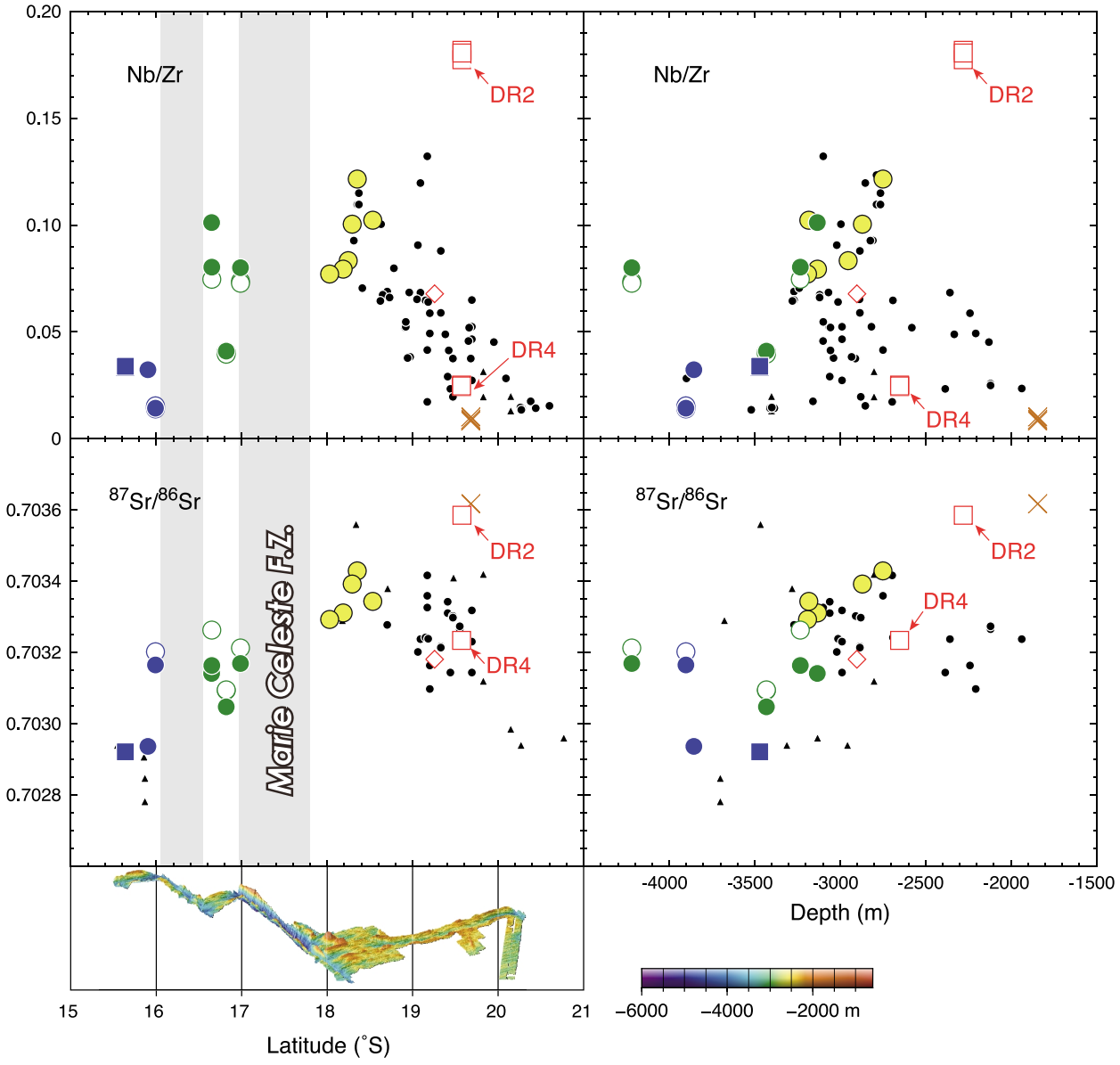

Fig. 8. Latitudinal distribution and correlation with water depth of Nb/Zr and $^{87}Sr/^{86}Sr$ values for basalts from the Central Indian Ridge and Gasitao Ridge, showing correlation between along-ridge geochemical variation and bathymetry features. Symbols as in Fig. 2. Bathymetric data and color scale as in Fig. 1b.

(Fig. 8). The influence of RE2 decreases along with decreasing magma production to the north. That influence is unidentifiable in basalt from the northern part of Segment 18. This observation also indicates that the MCFZ does not influence compositional change. Although the influence of RE2 decreases somewhat southward, basalts with extreme RE2 signatures were produced in the center parts of Segment 15, where the shallow ridge bathymetry suggests that magma production is high (Fig. 8). In contrast to RE2, the geochemical signature of RD in basalt is geographically limited to two places: the south end of Segment 18 and the center part of Segment 15 (Fig. 8). However, these observations reveal that both RE2 and RD contribute strongly to magma production on Segment 15.

Ternary Connection along the Central Indian Ridge: magma chemistry, crustal volume, and scale of regional source heterogeneity If the heterogeneity is small-scale, then melt derived from enriched material will be diluted by depleted melt produced by surrounding peridotite melting (Meibom and Anderson, 2003; Machida *et al.*, 2009). In this scenario, the magma composition will be

less enriched in trace elements. Moreover, the isotopic ratios will not become radiogenic. Our report describes actually huge sheet flows extending through the axial valley around site RC10 at the center of Segment 16. These flows, called the "Great Dodo Lava Plain", were identified using the Autonomous Underwater Vehicle (AUV) r2D4 during the KH06-04 cruise (Ura *et al*., 2007). Such a sheet flow shows a high effusion rate (Head *et al*., 1996). However, our observations show that basalts from Segment 16 have enriched trace element concentrations, and have radiogenic isotopic signatures resulting from the contribution of RE2. This evidence suggests that geochemical enrichment corresponds to the quantity of melt production. The appearance of the geochemical influence of enriched material in magma compositions in spite of dilution by surrounding-peridotite-derived (depleted) melt indicates the existence of quite large-scale plume-unrelated heterogeneity (source for RE2) under Segment 16.

The same argument can be extended to Segment 15. Large crustal volume along Segment 15 can be interpreted by melting of the source for RE2 and RD (Figs. 5 and 6), as discussed previously. The across-ridge variation in Segment 15C (figure 3 of Cordier *et al*. (2010)) can be reinterpreted by considering the contribution of RD (Gasitao Ridge) for Group-1, and RE2 (Rodrigues Ridge) for Group-2. Data suggests that these two components coexisted beneath Segment 15 for the last 800 kyr. However, along-axis variation (Fig. 8) shows that the influence of RE2 decreases toward the center of Segment 15. The volcanic morphology of site DR2 (Fig. 9) implies limited influence of RE2 because small shield-like morphological features indicate a lower effusive rate (Head *et al*., 1996). In contrast, site DR4 is situated on the linear axial volcanic ridge, indicating a higher effusion rate (Fig. 9). Therefore, melting of RD mainly regulates large crustal volumes at the center of Segment 15. However, the appearance of RD is restricted to the center of Segment 15 and the southern end of Segment 18 (Fig. 8). Therefore, we propose that RD is a small-scale heterogeneity, which will become discernable if the influence of RE2 decreases. We also infer that RD is regionally distributed because it has affected at least two separate segments.

Our geochemical investigations for MORB from CIR revealed that the diffusion of solid plume material is limited. No channelized flow takes place from the Réunion hotspot to CIR. We argue also that Segment 16 is the point on the ridge that is subject to the strongest influence from radiogenic materials consisting the upper mantle heterogeneity. Then, the simplest interpretation is that recycled materials are melted in large quantities. It appears that melting of ancient recycled plate materials with a low melting point rather than that of depleted peridotite (e.g., Olafsson and Eggler, 1983; Falloon and Green, 1990; Takahashi *et al*., 1998; Sobolev *et al*., 2007; Pilet *et al*., 2008) regulates the melt production volume.

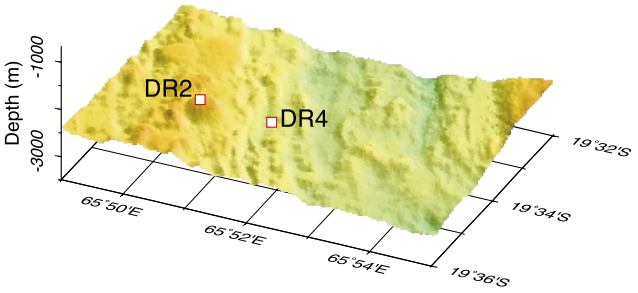

Fig. 9. Three-dimensional map portraying detailed topography of dredge sites DR2 and 4 at the center of Segment 15 viewed from S25°E. Bathymetric data and the color scale as in Fig. 1b.

Consistent interpretation of regional mantle heterogeneity around the Réunion hotspot and Central Indian Ridge

The Rodrigues and Gasitao (Three Magi) Ridges connect physiographically to a hot spot track (Fig. 1). However, they originate from RE2 and RD indicating regional mantle heterogeneity unrelated to the Réunion plume, as shown in Figs. 5 and 6, and as discussed previously. Therefore, we can infer that these volcanic edifices were formed by melting of recycled materials with a low melting point, and by exudation of magma along lithospheric tensional cracks (e.g., Forsyth *et al*., 2006; Hirano *et al*., 2006; Machida *et al*., 2009). Large-scale melting of RE2 source is necessary to form the large Rodrigues Ridge. In contrast, the small Gasitao Ridge might be derived from melting of a small-scale RD source heterogeneity. These considerations are consistent with our interpretation of the scale of regional heterogeneities as shown by the relation between the geochemical variation and the quantity of magma production along the CIR (Fig. 8). Therefore, the size of the Rodrigues and Gasitao ridges can also be interpreted as reflecting the scale of the heterogeneities they formed from in the underlying mantle. Furthermore, physiographical continuation of the Rodrigues and Gasitao ridges shows that RE2 and RD sources regionally coexist in the Indian Ocean mantle around the CIR and the Réunion hotspot. Both end members contribute to the magma generation on Segment 15 of the CIR, on the eastern extension of these ridges. Our findings support the theory that the Earth's upper mantle is heterogeneous because of the existence of plume-unrelated enriched materials of various scales and abundances (e.g., Zindler *et al*., 1984; Machida *et al*., 2009). Clarifying the scale and spatial distribution of these enriched or radiogenic components will contribute strongly

to our understanding of the nature of heterogeneity in the Indian Ocean mantle domain.

Conclusions

Geochemical investigations along the Rodrigues and neighboring segments of the CIR beyond the MCFZ clearly show that melt components of two kinds derived from different mantle materials unrelated to the Réunion plume (Radiogenic Enriched Component 2 (RE2; characterized by Rodrigues Ridge or Intermediate Series of Mauritius Island) and Radiogenic Depleted Component (RD; characterized by Gasitao Ridge)) mainly control the chemical signature of MORB. The peak for influence of these two components corresponds completely to shallow topography, indicating large magma volume. Therefore, we conclude that regional plume-unrelated upper mantle heterogeneity regulates melt production. Our results provide evidence for the limited diffusion of solid plume material. In the case of a mid-ocean ridge produced by melting of the large-scale heterogeneous Indian Ocean mantle domain, a substantial amount of melt would be created because of melting of recycled material with a lower melting point than that of the surrounding mantle peridotite. For the case of the distal ridge-hotspot interaction in the Indian Ocean mantle domain, we infer that the presence of an intra-plate ridge, even though it topographically connects the hotspot track and mid-ocean ridge, is insufficient evidence for channelized of plume flow.

Characteristics of the source for two radiogenic melt components (RE2 and RD) identified herein might advance our understanding of the origin and distribution of recycled material in the Indian Ocean mantle domain. However, these are beyond the scope of this paper. We believe that further unbiased investigations of other distal ridge-hotspot interactions with respect to upper mantle heterogeneity can reveal a universal distribution of two such radiogenic components, and can contribute greatly to our understanding of mantle recycling.

Acknowledgments—We gratefully acknowledge the shipboard scientific parties, captain, and crews of R/V Hakuho-maru for their efficient work, and T. Ura and A. Asada for helpful discussions of seafloor volcanic activity along the CIR during the KH06-04 cruise. We thank K. Okino for providing topographic data collected during the KH06-04 cruise. S.M. and M.T. are grateful to J. Matsuoka and K. Nagaishi for their invaluable assistance with Pb isotope analyses. S.W. would like to thank B. Murton, R. Williams, B. Jones, and J. Ford (NOC) for assistance with FTIR sample preparation and analysis. This study was performed as a cooperative research program of the Center for Advanced Marine Core Research (CMCR), Kochi University (Accept No. 09B038) with the support of JAMSTEC. This study was supported by JSPS grant-in-aid No. 21403012 (conceded to Y.O.), and Grant for Promotion of Niigata University Research Projects (conceded to N.N.). Instructive reviews and suggestions from P. Castillo and an anonymous reviewer contributed greatly to improvement of manuscript. We gratefully acknowledge T. Kogiso for handling of our manuscript and for helpful comments and suggestions. We also thank V. J. M. Salters and W. M. White for comments on an earlier manuscript. GMT software (Wessel and Smith, 1995) was used to display bathymetric data.

References

Albarède, F. and Tamagnan, V. (1988) Modelling the recent geochemical evolution of the Piton de la Fournaise volcano, Réunion Island. *J. Petrol.* **29**, 997–1030.

Albarède, F., Luais, B., Fitton, J. G., Semet, M., Kaminski, E., Upton, B. G. J., Bachèlery, P. and Cheminée, J.-L. (1997) The geochemical regimes of Piton de la Fournaise volcano (Réunion) during the last 530 000 years. *J. Petrol.* **38**, 171–201.

Backman, J., Duncan, R. A. *et al.* (1988) *Proc. ODP, Init. Repts.* **115**, College Station, TX (Ocean Drilling Program).

Baxter, A. N. (1990) Major and trace element variations in basalts from Leg 115. *Proc. ODP, Sci. Res.* (Duncan, R. A., Backman, J., Peterson, L. C. *et al.* eds.), **115**, 11–21, College Station, TX (Ocean Drilling Program).

Baxter, A. N., Upton, B. G. J. and White, W. M. (1985) Petrology and geochemistry of Rodrigues Island, Indian Ocean. *Contrib. Mineral. Petrol.* **89**, 90–101.

Blichert-Toft, J., Agranier, A., Andres, M., Kingsley, R., Schilling, J.-G. and Albarède, F. (2005) Geochemical segmentation of the Mid-Atlantic Ridge north of Iceland and ridge—hot spot interaction in the North Atlantic. *Geochem. Geophys. Geosyst.* **6**, Q01E19, doi:10.1029/2004GC000788.

Chauvel, C. and Hémond, C. (2000) Melting of a complete section of recycled oceanic crust: Trace element and Pb isotopic evidence from Iceland. *Geochem. Geophys. Geosyst.* **1**, doi:10.1029/1999GC000002.

Cherniak, D. J. (1998) Pb diffusion in clinopyroxene. *Chem. Geol.* **150**, 105–117.

Colin, A., Burnard, P. G., Graham, D. W. and Marrocchi, Y. (2011) Plume-ridge interaction along the Galapagos Spreading Center: discerning between gas loss and source effects using neon isotopic compositions and ^{4}He–$^{40}Ar^{*}$–CO_2 relative abundances. *Geochim. Cosmochim. Acta* **75**, 1145–1160.

Cordier, C., Benoit, M., Hémond, C., Dyment, J., Le Gall, B., Briais, A. and Kitazawa, M. (2010) Time scales of melt extraction revealed by distribution of lava composition across a ridge axis. *Geochem. Geophys. Geosyst.* **11**, Q0AC06, doi:10.1029/2010GC003074.

Cushman, B., Sinton, J., Ito, G. and Dixon, J. E. (2004) Glass compositions, plume-ridge interaction, and hydrous melting along the Galapagos Spreading Center, 90.5° to 98°W. *Geochem. Geophys. Geosyst.* **5**, Q08E17, doi:10.1029/2004GC000709.

Detrick, R. S., Sinton, J. M., Ito, G., Canales, J. P., Behn, M., Blacic, T., Cushman, B., Dixon, J. E., Graham, D. W. and Mahoney, J. J. (2002) Correlated geophysical, geochemical, and volcanological manifestations of plume-ridge interac-

tion along the Galapagos Spreading Center. *Geochem. Geophys. Geosyst.* **3**, 8501, doi:10.1029/2002GC000350.

Dupré, B. and Allègre, C. J. (1983) Pb–Sr isotope variation in Indian Ocean basalts and mixing phenomena. *Nature* **303**, 142–146.

Dyment, J., Lin, J. and Baker, E. T. (2007) Ridge-hotspot interactions. *Oceanography* **20**, 102–115.

Eggins, S. M., Woodhead, J. D., Kinsley, L. P. J., Mortimer, G. E., Sylvester, P., McCulloch, M. T., Hergt, J. M. and Handler, M. R. (1997) A simple method for the precise determination of ≥40 trace elements in geological samples by ICPMS using enriched isotope internal standardisation. *Chem. Geol.* **134**, 311–326, doi:10.1016/S0009-2541(96)00100-3.

Falloon, T. J. and Green, D. H. (1990) Solidus of carbonated fertile peridotite under fluid-saturated conditions. *Geology* **18**, 195–199.

Ferreira, P. L. (2006) Melt supply and magmatic evolution at a large central MOR volcano located in the Lucky Strike segment, 37°N on the Mid-Atlantic Ridge, Azores region. Dr. Sci. Thesis, Univ. Southampton, U.K.

Fisk, M. R., Upton, B. G. J., Ford, C. E. and White, W. M. (1988) Geochemical and experimental study of the genesis of magmas of Reunion Island, Indian Ocean. *J. Geophys. Res.* **93**, 4933–4950.

Forsyth, D. W., Harmon, N., Scheirer, D. S. and Duncan, R. A. (2006) Distribution of recent volcanism and the morphology of seamounts and ridges in the GLIMPSE study area: Implications for the lithospheric cracking hypothesis for the origin of intraplate, non-hot spot volcanic chains. *J. Geophys. Res.* **111**, B11407, doi:10.1029/2005JB004075.

Fretzdorff, S. and Haase, K. M. (2002) Geochemistry and petrology of lavas from the submarine flanks of Reunion Island western Indian Ocean: Implications for magma genesis and the mantle source. *Mineral. Petrol.* **75**, 153–184, doi:10.1007/s007100200022.

Füri, E., Hilton, D. R., Murton, B. J., Hémond, C., Dyment, J. and Day, J. M. D. (2011) Helium isotope variations between Réunion Island and the Central Indian Ridge (17°–21°S): New evidence for ridge-hot spot interaction. *J. Geophys. Res.* **116**, B02207, doi:10.1029/2010JB007609.

Graham, D. W., Christine, D. M., Harpp, K. S. and Lupton, J. E. (1993) Mantle plume Helium in submarine basalts from the Galapagos platform. *Science* **262**, 2023–2026.

Hanyu, T., Dunai, T. J., Davies, G. R., Kaneoka, I., Nohda, S. and Uto, K. (2001) Noble gas study of the Reunion hot spot: evidence for distinct less-degassed mantle sources. *Earth Planet. Sci. Lett.* **193**, 83–98, doi:10.1016/S0012-821X(01)00489-7.

Head, J. W., III, Wilson, L. and Smith, D. K. (1996) Mid-ocean ridge eruptive vent morphology and substructure: Evidence for dike widths, eruption rates, and evolution of eruptions and axial volcanic ridges. *J. Geophys. Res.* **101**, 28265–28280.

Hirano, N., Takahashi, E., Yamamoto, J., Abe, N., Ingle, S. P., Kaneoka, I., Hirata, T., Kimura, J.-I., Ishii, T., Ogawa, Y., Machida, S. and Suyehiro, K. (2006) Volcanism in response to plate flexure. *Science* **313**, 1426–1428, doi:10.1126/science.1128235.

Ingle, S., Ito, G., Mahoney, J. J., Chazey, W., III, Sinton, J., Rotella, M. and Christie, D. M. (2010) Mechanisms of geochemical and geophysical variations along the western Galápagos Spreading Center. *Geochem. Geophys. Geosyst.* **11**, Q04003, doi:10.1029/2009GC002694.

Ito, G., Lin, J. and Graham, D. (2003) Observational and theoretical studies of the dynamics of mantle plume-mid-ocean ridge interaction. *Rev. Geophys.* **41**, 1017, doi:10.1029/2002RG000117.

Jackson, M. G. and Dasgupta, R. (2008) Compositions of HIMU, EM1, and EM2 from global trends between radiogenic isotopes and major elements in ocean island basalts. *Earth Planet. Sci. Lett.* **276**, 175–186, doi:10.1016/j.epsl.2008.09.023.

Kelemen, P. B., Yogodzinski, G. M. and Scholl, D. W. (2003) Along-strike variation of the Aleutian Island Arc: Genesis of High Mg# andesite and implication for continental crust. *Inside the Subduction Factory* (Eiler, J., ed.), *Geophys. Monogr.* **138**, 223–276, AGU, Washington, D.C.

Kushiro, I. (1994) Recent experimental studies on partial melting of mantle peridotites at high pressures using diamond aggregates. *J. Geol. Soc. Japan* **100**, 103–110.

Le Bas, M. J., Le Maitre, R. W., Streckeisen, A. and Zanettin, B. (1986) A chemical classification of volcanic rocks on the total alkali-silica diagram. *J. Petrol.* **27**, 745–750.

Machida, S., Hirano, N. and Kimura, J.-I. (2009) Evidence for recycled plate material in Pacific upper mantle unrelated to plumes. *Geochim. Cosmochim. Acta* **73**, 3028–3037, doi:10.1016/j.gca.2009.01.026.

Magnani, M., Fujii, T., Orihashi, Y., Yasuda, A., Hirata, T., Santo, A. and Vaggrlli, G. (2006) Evidences of primitive melt heterogeneities preserved in plagioclase-hosted melt inclusions of South Atlantic MORB. *Geochem. J.* **40**(3), 277–290.

Mahoney, J. J., Natland, J. H., White, W. M., Poreda, R., Bloomer, S. H. and Baxter, A. N. (1989) Isotopic and geochemical provinces of the Western Indian Ocean spreading centers. *J. Geophys. Res.* **94**, 4033–4052.

McDonough, W. F. and Sun, S.-S. (1995) The composition of the Earth. *Chem. Geol.* **120**, 223–253.

Meibom, A. and Anderson, D. L. (2003) The statistical upper mantle assemblage. *Earth Planet. Sci. Lett.* **217**, 123–139, doi:10.1016/S0012-821X(03)00573-9.

Moore, J., White, W. M., Paul, D., Duncan, R. A., Abouchami, W. and Galer, S. J. G. (2011) Evolution of shield-building and rejuvenescent volcanism of Mauritius. *J. Volcanol. Geotherm. Res.* **207**, 47–66, doi:10.1016/j.jvolgeores.2011.07.005.

Morgan, W. J. (1978) Rodrigues, Darwin, Amsterdam. A second type of hotspot island. *J. Geophys. Res.* **83**, 5355–5360.

Murton, B. J., Taylor, R. N. and Thirlwall, M. F. (2002) Plume-ridge interaction: Geochemical perspective from the Reykjanes Ridge. *J. Petrol.* **43**, 1987–2012.

Murton, B. J., Tindle, A. G., Milton, J. A. and Sauter, D. (2005) Heterogeneity in southern Central Indian Ridge MORB: implications for ridge—hot spot interaction. *Geochem. Geophys. Geosyst.* **6**, Q03E20, doi:10.1029/2004GC000798.

Nakamoto, K. (1997) *Infrared and Raman Spectra of Inorganic and Coordination Compounds*. 5th ed., Wiley, New York.

Nauret, F., Abouchami, W., Galer, S. J. G., Hofmann, A. W., Hémond, C., Chauvel, C. and Dyment, J. (2006) Correlated trace element-Pb isotope enrichments in Indian MORB along 18–20°S, Central Indian Ridge. *Earth Planet. Sci. Lett.* **245**, 137–152, doi:10.1016/j.epsl.2006.03.015.

Nohda, S., Kaneoka, I., Hanyu, T., Xu, S. and Uto, K. (2005) Systematic variation of Sr-, Nd- and Pb-isotopes with time in lavas of Mauritius, Réunion hot spot. *J. Petrol.* **46**, 505–522, doi:10.1093/petrology/egh085.

Olafsson, M. and Eggler, D. H. (1983) Phase relations of amphibole, amphibole-carbonate, and phlogopite-carbonate peridotite: petrologic constraints on the asthenosphere. *Earth Planet. Sci. Lett.* **64**, 305–315.

Parman, S. W., Kelley, S. P., Ballentine, C. J. and van Orman, J. A. (2009) Partitioning and diffusion of noble gases in olivine at mantle pressures. *Geochim. Cosmochim. Acta* **73**, A995–A995.

Paul, D., White, W. M. and Blichert-Toft, J. (2005) Geochemistry of Mauritius and the origin of rejuvenescent volcanism on oceanic island volcanoes. *Geochem. Geophys. Geosyst.* **6**, Q06007, doi:10.1029/2004GC000883.

Pearce, N. J. G., Perkins, W. T., Westgate, J. A., Gotron, M. P., Jackson, S. E., Neal, C. R. and Chenery, S. P. (1997) A compilation of new and published major and trace element data for NIST SRM 610 and NIST SRM 612 glass reference materials. *Geostand. Newslett.* **21**, 115–144.

Peng, Z. X. and Mahoney, J. J. (1995) Drillhole lavas from the northwestern Deccan Traps, and the evolution of Reunion hotspot mantle. *Earth Planet. Sci. Lett.* **134**, 169–185.

Pilet, S., Baker, M. B. and Stolper, E. M. (2008) Metasomatized lithosphere and the origin of alkaline lavas. *Science* **320**, 916–919, doi:10.1126/science.1156563.

Salters, V. J. M. and Stracke, A. (2004) Composition of the depleted mantle. *Geochem. Geophys. Geosyst.* **5**, doi:10.1029/2003GC000597.

Schilling, J.-G., Kingsley, R. H. and Devine, J. D. (1982) Galapagos hot spot-spreading center system 1. Spatial petrological and geochemical variations (83°W–101°W). *J. Geophys. Res.* **87**, 5593–5610.

Sheth, H., Mahoney, J. J. and Baxter, A. (2003) Geochemistry of lavas from Mauritius, Indian Ocean: Mantle sources and Petrogenesis. *Int. Geol. Rev.* **45**, 780–797, doi:10.2747/0020-6814.45.9.780.

Sneeringer, M., Hart, S. R. and Shimizu, N. (1984) Strontium and samarium diffusion in diopside. *Geochim. Cosmochim. Acta* **48**, 1589–1608.

Sobolev, A. V., Hofmann, A. W., Kuzmin, D. V., Yaxley, G. M., Arndt, N. T., Chung, S.-L., Danyushevsky, L. V., Elliott, T., Frey, F. A., Gracia, M. O., Gurenko, A. A., Kamenetsky, V. S., Kerr, A. C., Krivolutskaya, N. A., Matvienkov, V. V., Nikogosian, I. K., Rocholl, A., Sigurdsson, I. A., Sushchevskaya, N. M. and Teklay, M. (2007) The amount of recycled crust in sources of mantle-derived melts. *Science* **316**, 412–417, doi:10.1126/science.1138113.

Takahashi, E., Nakajima, K. and Wright, T. L. (1998) Origin of the Columbia River basalts: melting model of a heterogeneous plume head. *Earth Planet. Sci. Lett.* **162**, 63–80.

Takahashi, T. and Shuto, K. (1997) Major and trace element analyses of silicate rocks using X-ray fluorescence spectrometry RIX3000. *Rigaku-Denki J.* **28**, 25–37 (in Japanese).

Takazawa, E., Okayasu, T. and Satoh, K. (2003) Geochemistry and origin of the basal lherzolites from the northern Oman ophiolite (northern Fizh block). *Geochem. Geophys. Geosyst.* **4**, 8605, doi:10.1029/2001GC000232.

Tanimizu, M. and Ishikawa, T. (2006) Development of rapid and precise Pb isotope analytical techniques using MC-ICP-MS and new results for GSJ rock reference samples. *Geochem. J.* **40**, 121–133.

Trull, T. W. and Kurz, M. D. (1993) Diffusivity of ^{3}He and ^{4}He in olivine and clinopyroxene at magmatic and mantle temperatures. *Geochim. Cosmochim. Acta* **57**, 1313–1324.

Ura, T., Tamaki, K., Asada, A., Okamoto, K., Nagahashi, K., Sakamaki, T., Gamo, T., Okino, K., Obara, T., Nakane, K., Obata, T., Ooyabu, Y., Yamaoka, N., Orihashi, Y., Han, J., Koyama, H. and Sugimatsu, H. (2007) Daives of AUV "r2D4" to rift valley of Central Indian Mid-Ocean ridge system. *OCEAN's 07*, Aberdeen, UK, Jan. 23, Proc. 004, 1–6.

Van Orman, J. A., Grove, T. L. and Shimizu, N. (2001) Rare earth element diffusion in diopside: influence of temperature, pressure, and ionic radius, and an elastic model for diffusion in silicates. *Contrib. Mineral. Petrol.* **141**, 687–703.

Wessel, P. and Smith, W. H. F. (1995) New version of the generic mapping tools released. *Eos Trans. AGU* **76**, 329.

White, W. M., Cheatham, M. M. and Duncan, R. A. (1990) Isotope geochemistry of Leg 115 basalts and inferences on the history of the Reunion mantle plume. *Proc. ODP, Sci. Res.* (Duncan, R. A., Backman, J., Peterson, L. C. *et al.*, eds.), **115**. 53–61, College Station, TX (Ocean Drilling Program).

Workman, R. K. and Hart, S. R. (2005) Major and trace element composition of the depleted MORB mantle (DMM). *Earth Planet. Sci. Lett.* **231**, 53–72, doi:10.1016/j.epsl.2004.12.005.

Zindler, A., Staudigel, H. and Batiza, R. (1984) Isotope and trace element geochemistry of young Pacific seamounts: implications for the scale of upper mantle. *Earth Planet. Sci. Lett.* **70**, 175–195.

SUPPLEMENTARY MATERIALS

URL (http://www.terrapub.co.jp/journals/GJ/archives/data/48/MS320.html)
Figures S1 to S9, Tables S1 to S3: MS320.pdf
Command Script A: script_for_Sr-Nd-7Pb-plot.txt
Command Script B: script_for_6-7-8Pb-plot.txt
Loading data: Data-CIR&Reunion.txt
Movie A: Fig.S10_CIR-Reunion_Sr-Nd-7Pb.mp4
Movie B: Fig.S11_CIR-Reunion_6-7-8Pb.mp4